Divergences in the control of mitochondrial respiration are associated with lifespan variation in marine bivalves

Enrique Rodríguez[1](MSc.), Mohammed Hakkou[1](BSc.), Tory M. Hagen[2](Ph.D), Hélène Lemieux[3](Ph.D), and Pierre U. Blier[1](Ph.D)

1. Département de Biologie, Université du Québec, 300 des Ursulines, Rimouski, Québec, Canada, G5L 3A1
2. Linus Pauling Institute, Oregon State University 335 Linus Pauling Science Center Corvallis, OR 97331, USA
3. Faculty Saint-Jean, Dept. of Medicine, Women and Children Health Research Institute, University of Alberta, Edmonton, Alberta

Address of the author for correspondence: Pierre Blier, Département de Biologie, Université du Québec, 300 des Ursulines, Rimouski, Québec, Canada, G5L 3A1, Phone : +1-418-723-1986, fax : +1-418-724-1849, email: pierre_blier@uqar.ca

Abstract

The role played by mitochondrial function in the aging process has been a subject of intense debate in the past few decades, as part of the efforts to understand the mechanistic basis of longevity. The mitochondrial oxidative stress theory of aging (MOSTA) suggests that a progressive decay of this organelle's function leads to an exacerbation of oxidative stress, with deleterious impact on mitochondrial structure and DNA, ultimately promoting aging. Among the traits suspected to be associated with longevity is the variation in regulation of oxidative phosphorylation, potentially impacting the management of oxidative stress. Longitudinal studies using the framework of metabolic control analysis have shown age-related differences in flux control of respiration, but this approach has seldom been taken on a comparative scale. Using four species of marine bivalves exhibiting a large range of maximum lifespans (from 28y to 507y), we report lifespan-related differences in flux control at different steps of the electron transfer system. Increased longevity was characterized by a lower control by NADH- (complex I-linked) and Succinate- (complex II- linked) pathways, while respiration was strongly controlled by complex IV when compared to shorter-lived species. Complex III exerted a strong control over respiration in all species. Furthermore, high longevity was associated with higher citrate synthase activity, and lower ATP synthase activity. Relieving the control exerted by the electron entry pathways could be advantageous for reaching a higher longevity, leading to an increased control by complex IV, the final electron acceptor in the electron transfer system.

Keywords: Mitochondria, Metabolism, Longevity, Invertebrate

Introduction

The fundamental mechanisms associated with longevity have captivated ancient philosophers and modern biologists alike, and their intricacies are still subject to intense debate. Mounting evidence from longitudinal and comparative studies point toward mitochondrial structure and function, particularly the electron transfer system (ETS) and its involvement in reactive oxygen species (ROS) production. The mitochondrial oxidative stress theory of aging (MOSTA) posits that ROS-induced damage to lipids, proteins, and mitochondrial DNA ultimately leads to the accumulation of dysfunctional macromolecules and attendant deficits in mitochondrial function. Accumulation of oxidative damage is not only associated with ROS appearance but also with attenuated repair mechanisms and species-dependent loss of antioxidant defenses (1, 2). Ultimately, a vicious cycle of increasing damage leading to morbidities and mortality ensues (reviewed in (3)). Despite suffering from criticism often linked to the role of antioxidants and ROS in cellular function (4), evidence points toward a link between mitochondrial membrane resistance to oxidative insult, regulation of ROS, mtDNA damage control, and lifespan in a variety of species (1, 5).

Recent support of the MOSTA comes from studies comparing the longest-lived non-colonial metazoan, the ocean quahog *A. islandica*, to other shorter-living marine bivalves. *A. islandica* has maximum reported longevity (MRL) of 507 years in the North Atlantic (6). This longevity is far above the MRLs of three closely related and similar-sized species: *Mya arenaria* (28 y), *Spisula solidissima* (37 y), and *Mercenaria mercenaria* (106 y). The ocean quahog's case of extreme longevity comes with a more peroxidation-resistant mitochondrial membrane and lower ROS production (measured as H_2O_2 efflux) compared to the other bivalves, but similar capacities for oxidative phosphorylation (OXPHOS, (7) and (8)). Interestingly, the low ROS production of *A. islandica* is not the result of low OXPHOS capacity or reduced protonmotive force, because it occurs in substrate conditions

associated with high respiratory coupling efficiency, i.e., high respiration rates and small proton leak. This suggests that this particular species has evolved not only an efficient stong antioxidant system (9), but also a mitochondrial phenotype where a low proportion of oxygen is diverted to ROS production. The exact mechanisms behind this feat, however, remain obscure.

A possible mechanism by which long-lived species may be able to maintain low rates of ROS production, without compromising respiration, maybe through a rearrangement of the stoichiometry of the ETS and the enzymes of the tricarboxylic acid cycle (TCA). Indeed, activities of ETS complexes normalized to mitochondrial content differed clearly between the short-lived *M. arenaria* and the long-lived *A. islandica*. The longest-lived species expressed markedly lower activities of Complexes I (NADH:ubiquinone oxidoreductase), I-III segment (coenzyme Q – cytochrome c oxidoreductase), and II (succinate dehydrogenase). At the same time, the authors measured similar activities of complex IV (cytochrome c oxidase, the terminal electron acceptor enzyme) among species. Complexes I and II are especially relevant as they are essential electron entry complexes of the NADH- and Succinate-pathways, respectively. Depending on the substrate oxidized, the flavin and quinone reduction sites of complex I (I_F and I_Q), and quinol oxidation site in complex III (III_{Qo}) are among the sites reaching maximal rates of superoxide production leading to maximal rates of H_2O_2 efflux. At the same time, evidence points to a substantial contribution of the flavin site at complex II (site II_F,(10)). Hence, the lower activities of complexes I, II, and complexes I-III segment in longer-lived species could entail a lower diversion of electrons to these ROS-producing sites and explain the lower rates of ROS production (11, 12).

Investigating the topologies of the ETS complexes and the enzymatic control of electron flow among species of diverging lifespans could prove useful to determine the mitochondria involvement in animal longevity (3). The framework of metabolic control analysis (MCA), which measures the specific control strength by a step in a pathway (see (13) and references therein), can be quite useful to perform these investigations. Increased control strength at a specific step indicates a higher

impact of changes in the activity at this step (14). This method has been useful in detecting mitochondrial dysfunctions in the context of pathologies and age-related diseases; a redistribution of control can reveal the onset of disease or development of aging (15). Complex I is often found as a determinant site: an increase in control by this step can induce OXPHOS dysfunction and mitochondrial ROS production (16-18). Nonetheless, the understanding of the regulatory mechanisms of OXPHOS under physiological conditions remains incomplete (19). To our knowledge, no comparative studies have investigated if the control of mitochondrial respiration could be related to lifespan differences among species. This potential association between respiration control and lifespan is an important issue as it could reveal a simple evolutionary mechanism allowing modulation of longevity.

We used the framework of metabolic control analysis to study the control of electron flux in the mitochondrial ETS and its possible link with lifespan in the mantle, a predominantly aerobic tissue composed of secretory, sensory and muscular cells (20). Here we predict that the distribution of control on respiration should diverge in longer-lived species. This prediction is based on the lower activity of the complexes and enzymes associated with electron entry in *A. islandica,* when compared to short-lived species *M. arenaria* (8).

Methods

Bivalve collection and mitochondrial isolation

Bivalve species were either sampled at low tide (*Mya arenaria*, *Mercenaria mercenaria*) or collected by professional divers (*Spisula solidissima, Arctica islandica*). They were maintained in flow-through tanks at 8 ºC for at least a month before experiments. Mature individuals within the

same narrow range of shell sizes were selected for the experiments, as done in previous studies (7, 8). Mitochondrial isolation was carried out as previously described (8) with a modified isolation buffer (21) in which KCl was replaced with NaCl. Approximately 8 g of mantle were pooled from 2-4 individuals, and rinsed in the isolation buffer (400 mM Sucrose, 70 mM HEPES, 50 mM NaCl, 6 mM EGTA, 3 mM EDTA, 10 mg/ml aprotinin, 1% [w/w] bovine serum albumin), minced and homogenized using a glass-Teflon potter on ice. The homogenate was centrifuged at 4 ºC twice at 1250 *g* for 10 min, and the supernatant was centrifuged at 10500 *g*. The resulting mitochondrial pellet was resuspended with a 0.5% BSA isolation buffer, centrifuged again and resuspended in about 500 µl of buffer per 4 g of tissue (wet weight). Protein concentration was immediately determined using the Biuret test before respirometry.

Pathway control of mitochondrial respiratory capacity

Mitochondrial respiration was quantified at 10 ºC using a substrate-uncoupler-inhibitor-titration (SUIT) protocol in an Oxygraph-2K (Oroboros Instruments Inc., Innsbruck, Austria). The maximal capacity of each specific pathway (NADH-, succinate-, or complex III-pathways) or step (complex IV) was measured under electron transfer (ET) state after uncoupling in one chamber of the O2k. Once the flux was stabilized to the maximal capacity, a titration with a specific inhibitor of the pathway or step was performed. Simultaneously, the effect of the same inhibitor titration was measured in the other chamber on the combined pathways flux under coupled OXPHOS state, with a total of 4-5 biological replicates per species and titration protocol. All the substrate concentrations were previously tested in bivalves to ensure saturation (maximal respiration rates). See fig. 1A for a schematic of the titration protocols, which are detailed hereafter.

Combined pathways flux under coupled OXPHOS state (NSGp-pathway)

Flux through the combined pathways was measured with successive addition of substrates feeding three pathways: NADH-pathway (25 mM glutamate and 2 mM malate), succinate-pathway

(10 mM succinate), and glycerol-3-phosphate-pathway (10 mM glycerol-3-phosphate). ADP (5 mM) was added immediately after the NADH-pathway substrates. The integrity of the outer mitochondrial membrane was diagnosed by adding cytochrome *c* (10 µM) after ADP. The specific inhibitor titration, as described for each pathway and steps below, was then applied to that maximal combined pathways flux.

NADH-pathway under ET state

The maximum NADH-pathway (N-pathway) capacity was measured in the presence of glutamate (25 mM), malate (2 mM) and ADP (5 mM). Uncoupling with an optimal concentration of FCCP was performed (final concentration between 0.5 and 0.75 µM) to ensure maximal flux through the pathway. Rotenone (0.01 – 600 nM) was then added in successive steps until maximal inhibition of the N-pathway.

Succinate-pathway under ET state

Succinate-pathway (S-pathway) was measured in the presence of succinate (10 mM), rotenone (1 µM) and ADP (5 mM). Maximum pathway capacity was obtained by a titration up to an optimum concentration of FCCP (0.5 - 0.75 µM). Inhibition of S-pathway was done by the successive addition of malonate (0.5 – 11 mM).

Complex III-pathway under ET state

Complex III-pathway was measured with ADP (5 mM) and reduced coenzyme Q_2 (CoQ_2H_2, 15 $\mu g.ml^{-1}$). Maximum CIII-driven ET capacity was obtained by a titration up to an optimal concentration of FCCP (0.5 - 0.75 µM). Inhibition was achieved through stepwise additions of antimycin A (1.25 nM – 3.31 µM).

Complex IV under ET state

Complex IV capacity was measured following the same protocol as in the combined pathways flux under coupled OXPHOS state (above), followed by titration with optimal FCCP concentration (0.5 - 0.75 µM; ET state), inhibition of complex III (2.5 µM antimycin A), alternative oxidase (100 µM n-propyl gallate), and complex I (1 µM rotenone), and addition of ascorbate (2 mM) and N,N,N',N'-Tetramethyl-p-phenylenediamine dihydrochloride (TMPD, 0.5 mM). Complex IV inhibition was done by titration with freshly prepared potassium cyanide (KCN, 0.05 – 102 µM).

Enzymatic activities of citrate synthase, CIV, and ATP synthase

Spectrophotometric measurements of the enzymatic activities were done on frozen aliquots of mitochondrial isolates from the same individuals used for the respirometry assays. CS and free CIV activities were measured at 10 ºC in a UV/VIS spectrophotometer (Ultrospec 2100 pro, Biochrom Ltd, Cambridge, UK) with an adapted version of the protocols established by Thibault, Blier (22). For the CIV assay, cytochrome *c* was reduced in 4.5 mM sodium dithionite. ATP synthase activity was measured using a modified version of the protocol developed by Barrientos, Fontanesi (23). The medium contained 250 mM sucrose, 20 mM HEPES and 5 mM $MgSO_4$ (pH 8.0) to which 0.35 mM NADH, 2.5 mM phosphoenolpyruvate, 2.5 mM ATP, 5 µM antimycin A, 4 units/ml each of lactate dehydrogenase and pyruvate kinase, and 3 µM oligomycin were added. The absorbance was read a 340 nm for 4 minutes.

Data analysis and calculation of flux control ratios

Datlab software was used for data analysis (Oroboros Instruments, Austria). Instrumental and chemical backgrounds were calibrated as a function of oxygen concentration and subtracted from the oxygen fluxes. Preliminary experiments validated the replacement of KCl by NaCl in the isolation buffer and the quality of mitochondrial isolates obtained, as respiration never increased over the 15% threshold upon cyt*c* addition (*A. islandica* NaCl = 10.39% [5.37-14.01], KCl = 6.32% [0.94-11.78]; *M. arenaria* NaCl = 1.06% [0-2.37], KCl = 5.87% [0-14.92]; n=4 per species).

We calculated flux control coefficients for each individual and species as the ratio of the initial slope of the global flux (J) over the initial slope of the isolated pathway activity (v_i) titrated with inhibitor I $\frac{(\frac{dJ/J}{dI})}{(\frac{dvi/vi}{dI})}$ (13).

Statistical analyses

Differences between groups were assessed via ANOVAs with Tukey's post-hoc HSD using Systat v. 13 (Systat Software, San Jose, CA). Variables were first tested for normality using the Shapiro-Wilk test. Figures were made using Sigmaplot v.12 (Systat Software, San Jose, CA) and Statistica 64 (Statsoft, Tulsa, OK).

Results

Pathway control of mitochondrial respiratory capacity

We measured respiration in mantle mitochondrial isolates using a SUIT protocol and calculated the flux control ratios (FCRs) normalized for maximal uncoupled respiration (ET capacity). Because the FCRs of the various steps did not significantly differ among species, we grouped the median responses for all four species in fig. 1B. The FCR for the N-pathway was 0.38 (0.24-0.87). Adding the succinate pathway to the N-pathway had a strong stimulatory effect on respiration, reaching a FCR of 0.56 (0.43-0.93). The effect was even stronger by the addition of the Gp pathway ($NSGp_P$), with a FCR of 1.00 (0.38-1.34). The addition of the uncoupler FCCP produced either very little or no increase in respiration, suggesting low or no limitation of OXPHOS by the phosphorylation system (ATP synthase, ADP/ATP transport, or phosphate carrier) in these bivalves. The contributions

of N-, S- and Gp-pathways in the OXPHOS state, calculated as N/NSGp, NS-N/NSGp, and NSGp-NS/NSGp, are detailed in fig. 1C. *M. arenaria* and *S. solidissima* display a significantly higher N-pathway contribution compared to either *M. mercenaria* or *A. islandica* (MA vs AI: p = 0.008; SS vs AI: p = 0.016; MA vs MM: p = 0.001; SS vs MM: p = 0.003). The S-pathway contribution to maximal OXPHOS was similar among all species. The Gp-pathway contribution was stronger in *A. islandica* and *M. mercenaria* compared to *S. solidissima* (p = 0.016 and 0.008, respectively).

N-pathway. Titration with rotenone to inhibit the N-pathway had different effects on NSGp-sustained flux among species (Fig. 2A and and detailed in fig. S1). The threshold plots display the NSGp-pathway flux as a function of the relative inhibition of the N-pathway. Calculated flux control coefficients for the N-pathway were 0.41±0.12 for *M. arenaria*, 0.41±0.06 for *S. solidissima*, 0.52±0.1 for *M. mercenaria*, and 0.04±0.01 for *A. islandica*. The N-pathway thus showed markedly lower control over NSGp-driven respiration in *A. islandica* compared with the 3 other species (Tukey's post-hoc test p = 0.047 between *A. islandica vs. M. arenaria* and *S. solidissima* and p = 0.007 between *A. islandica vs. M. mercenaria*). At maximal N-pathway inhibition, OXPHOS capacity of the NSGp–pathway was inhibited by 11% in *A. islandica*, while it was inhibited by up to 58% in *S. solidissima*.

S-pathway. Inhibition of the succinate pathway with malonate (Fig. 2B and detailed in fig. S2) had different effects on NSGp-sustained flux among species. Calculated flux control coefficients for S-pathway were 0.15±0.01 for *M. arenaria*, 0.42±0.04 for *S. solidissima*, 0.25±0.06 for *M. mercenaria*, and 0.05±0.01 for *A. islandica*. S-pathway in *A. islandica* had lower control over combined pathway OXPHOS capacity (NSGp) compared to *S. solidissima* (Tukey's post-hoc test $p \leq$ 0.001) or *M. mercenaria* (p = 0.007), but not compared to *M. arenaria* (p = 0.422). Flux control coefficient for the succinate pathway was significantly higher in *S. solidissima* compared to both *M. arenaria* (p = 0.001) and *M. mercenaria* (p = 0.042). At maximal S-pathway inhibition, combined OXPHOS pathway flux (NSGp) was inhibited by 11% in *A. islandica*, while it was inhibited by 43% in *S.*

solidissima. Fig. S5 shows N- and S-oxidative phosphorylation pathways capacity normalized by maximal N and S uncoupled pathways in isolated runs for each pathway. The flux through the N-pathway did not vary among species and was lower than the maximal ET flux. Nevertheless, the flux through the S-pathway (when succinate is the only substrate and Complex I is inhibited) was significantly closer to maximal uncoupled capacity in *A. islandica* (1.11±0.06) and *M. mercenaria* (1.00±0.03) compared to the two shorter-lived species (0.55±0.1 and 0.62±0.03 for *S. solidissima* and *M. arenaria*, respectively; $p < 0.05$). Inside species, no difference was found between both pathways' for short-lived bivalves, whereas S-pathway during oxidative phosphorylation was much closer to the maximal uncoupled capacity than the N-pathway in *A. islandica* (1.11±0.06 vs. 0.74±0.04; $p = 0.028$) and *M. mercenaria* (1.00±0.03 vs. 0.68±0.06).

Complex III-pathway. Titration of complex III by Antimycin A (Fig. S3) had a substantial effect on the NSGp-sustained flux among species. Calculated flux control coefficients for CIII were 0.76±0.1 for *M. arenaria*; 0.92±0.05 for *S. solidissima*; 0.90±0.13 for *M. mercenaria*, and 0.91±0.1 for *A. islandica*. No statistically significant differences were found among species for the control of respiration by CIII.

Complex IV. Cyanide titration of complex IV had different effects on NSGp-sustained flux among species (Fig. 3 and detailed in fig. S4). Calculated flux control coefficients for complex IV and initial linear regressions were 0.25±0.09 for *M. arenaria* [$y = 0.962 – (0.354x)$; $r^2=0.75$]; 0.19±0.04 for *S. solidissima* [$y = 1.015 – (0.324x)$; $r^2=0.9$]; 0.46±0.08 for *M. mercenaria* [$y = 1.009 – (0.457x)$; $r^2=0.97$], and 0.70±0.05 for *A. islandica* [$y = 0.975 – (0.633x)$; $r^2=0.97$]. Complex IV in *A. islandica* exerted a higher control over combined OXPHOS pathways flux (NSGp) compared to *S. solidissima* (Tukey's post-hoc test $p = 0.001$) and *M. arenaria* ($p = 0.002$), and a trend for a higher, albeit non-statistically significant, control compared to *M. mercenaria* ($p = 0.103$). Complex IV excess capacity (CIV_E/NSGp flux ratio), calculated as the intercept at zero complex IV inhibition of a linear regression through the points after the inhibition threshold varied among species: *M. arenaria* = 2.404 (1.110-

3.847), *S. solidissima* = 3.106 (1.771-4.256), *M. mercenaria* = 2.224 (1.305-3.865), *A. islandica* = 1.339 (1.065-1.637); $r^2 \geq 0.8$ for all species. Fig. S6 shows the activities of each pathway combined, normalized by maximal ET state. Whereas N-pathway activity did not vary significantly among species, the combined NS-pathway activity was significantly higher in *S. solidissima* (0.60±0.17) compared to *M. arenaria* and *A. islandica* (0.51±0.04 and 0.50±0.03; $p < 0.05$), but not to *M. mercenaria* (0.57±0.04). Similarly, NSGp-pathway activity was significantly higher in *S. solidissima* (1.06±0.16) than in *M. arenaria* and *A. islandica* (0.81±0.03 and 0.89±0.08; $p < 0.05$), but not *M. mercenaria* (1.01±0.02). Inside species, sequential addition of S- and Gp-pathway substrates significantly elevated activity comparatively to the previous step ($p < 0.05$ for all comparisons), except for the addition of Gp-pathway substrates in *S. solidissima* compared to NS-pathway.

Sum of flux control coefficients. Fig. 4 shows the control coefficients calculated for N-, S-, CIII- pathways and CIV single step (and sums thereof) in each species (*n = 4-5* individuals per pathway/step and species), as explained above. It showed significant ($p < 0.05$) differences among species. The sum of single step control coefficients varied between *M. arenaria* (1.57) and *M. mercenaria* (2.13).

Enzymatic activities of CS, CIV and ATPase. Fig. S7 shows the activities of 3 key enzymes in mitochondrial aliquots of the same individuals used for the high-resolution respirometry runs. CS activity (in U by mg of mitochondrial proteins) was significantly higher in longer-lived *M. mercenaria* and *A. islandica* (0.28±0.05 and 0.28±0.02 respectively) than in the shorter-lived species *M. arenaria* and *S. solidissima* (0.10±0.01 and 0.08±0.04; $p < 0.05$). CIV activity (normalized by mg of mitochondrial proteins) was significantly higher in *A. islandica* than *M. arenaria* (0.007±0.02 vs 0.001±0.0003; $p = 0.028$), but not significantly different between other species. ATPase activity, when normalized by CS was lower in the longer-lived species *M. mercenaria* and *A. islandica* (0.1±0.04 and 0.05±0.01) compared to the shorter-lived species *M. arenaria* and *S. solidissima* (0.45±0.13 and 0.28±0.03; $p < 0.05$). When normalized by CIV activity, ATPase activity remained

significantly higher in *M. arenaria* (20.02±2.49), but not *S. solidissima* (4.27±0.29), compared to longer-lived bivalves (9.33±0.89 for *M. mercenaria* and 3.24±0.89 for *A. islandica*; $p \leq 0.001$).

Discussion

We provide evidence for longevity-related differences in the control of respiration by the pathways and enzymatic complexes of the ETS in marine bivalves, a longevity model including the longest-lived non-colonial animal known to science. Using a novel approach with intact mitochondria, we found that the upstream electron entry pathways (NADH and succinate) exert a lower control on respiration in the extremely long-lived species *A. islandica*, when compared with three related species of shorter lifespans. Furthermore, longer lifespan species were characterized by a higher control of OXPHOS by the terminal electron-accepting enzyme complex IV, higher upstream contribution of the TCA cycle (in the form of CS activity), and a lower the ATP synthase activity (complex V) compared to shorter-lived species.

The N-pathway exerts less substantial control over combined pathways respiration in longer-lived than in shorter-lived species. Some insights from the literature support an advantage of a low contribution of the N-pathway or complex I to OXPHOS capacity to increase longevity. In seed beetles selected for their late reproduction and higher longevity, stronger resistance to the complex I inhibitor tebufenpyrad indicates of a lower dependence on the N-pathway for energy production, compared to shorter-lived and early reproducing individuals (24). In planarian flatworms, animals considered immortal (25), the contribution of the N-pathway to maximal OXPHOS capacity is minor compared to other species (26). All these results suggest that relieving part of the control exerted by the N-pathway (dependent on complex I) might give an advantage in terms of longevity. If complex I is a sensitive step that accumulates dysfunction during aging, it would be of interest for long-lived species to minimize control strength at this level. This could ensure that any alteration minimally impacts the overall oxidative capacity or fine regulation of respiration. In fact, experiments on *C.*

elegans support this assumption by showing that improving the structural stability of complex I leads to increased lifespan, improved mitochondrial function, and decreased oxidative stress (28).

In the long-lived *A. islandica,* the succinate pathway also exerted a significantly lower control of combined pathways respiration compared to two out of three shorter-lived species (excluding *M. arenaria)*. Munro et al. (8) reported a seven-fold lower ratio of complex II/complex IV activity in *A. islandica* compared to *M. arenaria*, and suggest that a lack of sensitivity of the S-pathway to malonate-mediated inhibition could help explain the low H_2O_2 production found for the longest-lived bivalve in the same study. Measuring the maximal catalytic activities of enzymes in homogenized mitochondria (as in (8)), however, yields different information than measuring respiration in the intact system (as in our study). Here, the link between complex II activity and control strength may depend on the elasticity of the complex to its substrate (see (15)). Indeed, while the relative contribution of the S-pathway in the present study was similar among species, the OXPHOS capacity in isolated runs was closer to maximal ETS capacity in *A. islandica* and *M. mercenaria* compared to the two shorter-lived species. Our current and previous results (8) suggest that the flux generated through the S-pathway in long-lived bivalves is reached with a lower relative catalytic capacity of complex II. Increasing evidence points to the S-pathway as an important regulator of mitochondrial ROS production given its role in both the ETS and TCA cycle (reviewed in (31)). Complex II is an important site for ROS production in rat skeletal muscle in both forward and reverse reactions (30), and increased longevity through methionine restriction was accompanied by a substantial decrease in this complex's concentration in rat liver (31), as is the case in long-lived strains of *Drosophila* (32). Much like with the N-pathway, we show that the S-pathway is less sensitive to inhibition in longer-lived species, suggesting that partial complex II dysfunction would result in a milder negative impact on overall respiration and ROS production.

The complex IV pathway exerted a higher control over coupled respiration in *A. islandica* than in shorter-lived bivalves, the first report of this kind. In contrast, CIV catalytic activity

(normalized by citrate synthase activity,a proxy of mitochondrial content) did not differ between *A. islandica* and *M. arenaria* (8), alluding to the above mentioned differences in methodological approaches. How might control by CIV impact attained longevity? This complex is known to play a role in the regulation and control of metabolic state (13, 33), and its own activity is regulated by the availability of substrates and cofactors such as NADH, ADP, oxygen and inorganic phosphate. Detection of cellular ATP levels and adjustment of ATP production to demand can be done by allosteric inhibition of the enzyme through binding of isoform IV-1 to ATP, which might keep the membrane potential at low values in conditions of high matrix ATP/ADP ratios, preventing excessive ROS production (discussed in (19), and see (36)). Limitation of the electron flow by CIV could keep the ubiquinone pool in a highly reduced state; ROS production at CIII could therefore be limited, since oxidized ubiquinone (rather than the fully reduced ubiquinone pool) stimulates superoxide formation by CIII (37). Several studies reported a decrease in both CIV activity and ATP producing capacity with age in vertebrates and invertebrates models (35, 36). Age-related changes in CIV activity should considerably impact oxidative capacities; it would be of interest to further evaluate how these changes vary longitudinally among individuals of bivalve species, and how differences in control affect rates of ROS efflux by upstream complexes.

We further measured the catalytic activity of TCA cycle enzyme citrate synthase as a means of evaluating the capacity of pathways upstream, as well as downstream of the electron transport system, by measuring ATP synthase activity. We found that longer-lived species display higher CS activity per mitochondrial protein. Thus, the capacity to generate reducing equivalents that enter the ETS could be critical in longer-lived bivalves, perhaps echoing the maintenance of a high CS activity throughout lifespan (37). However, this would need more investigation, as Munro et al. (1) found a lower CS activity in the naked mole-rat, a murine model of longevity, compared to mice. Furthermore, ATPase activity was lower in longer-lived species when normalized by CS activity in line with reports in *C. elegans* worms showing a positive effect of ATP synthase inhibiton on lifespan, although the mechanism, likely linked to mTOR activity, has not been fully elucidated (38).

Nonetheless, we show for the first time interspecies variation in ATPase activity linked to lifespan, a finding which warrants further investigations.

In this study, we measured respiration at NADH, succinate, and Gp-pathway fluxes at substrate and ADP concentrations ensuring saturation. The use of Gp as a substrate to ensure maximal saturation of the ETS was based on a series of preliminary experiments performed with various substrates combinations and on a previous bivalve study (39). We found differences among species in the contribution of this pathway to respiration, with a higher contribution in *A. islandica* and *M. mercenaria* compared to *S. solidissima*. The Gp-pathway of electron entry might thus be more critical in species having a lower relative N-pathway capacity, potentially helping to alleviate the reduction state of complex I, the electron "slips" to molecular oxygen, and ROS production. Gp is a physiologically relevant substrate in bivalves, as the mitochondrial glycerol-3-phosphate dehydrogenase (mG3PDH) reduces Gp derived from dihydroxyacetone phosphate (a metabolite from glycolysis), or from glycerol derived from triglyceride or diglyceride catabolism (40). Bivalves' diet mainly consists of phytoplankton (41), often rich in lipids, potentially explaining the high rates of respiration through the mG3PDH. Since this dehydrogenase is a site of ROS production (42), it will be of interest in the future to assess the rates of ROS production in the presence of Gp and compare it to the rates with other substrates combinations in these species. Studying this type of “alternative” pathway of electron transport is relatively novel, but brings forth the diversity of bioenergetic strategies in animals, and questions the classical view of a linear electron transport system and its associated beliefs (40). As such, the sum of the various flux control coefficients for the ETS complexes of marine bivalves found in this study is well over 1; this feat is reminiscent of the pivotal studies by Bianchi and colleagues, who also found this sum to be above unity, suggesting that they work as a single entity and providing some of the first evidence for supercomplex assemblies (43). The existence of these dynamic supramolecular assemblies is now well established: their composition, formation and stability appear to decrease with age (44), and they are thought to play roles in the regulation of electron flux, as well as in ROS production and longevity (46).

Pharmacological inhibition of their constituent complexes (especially of complex I) can disrupt their assembly and affect ROS efflux and ATP production (47). It is therefore conceivable that longer-lived species have less control (or less "sensitivity") at the level of complex I in order to avoid supercomplex breakdown and its detrimental consequences. This potential robustness of supercomplex assemblies and lower control of electron entry complexes over the ETS may also explain the maintenance of low rates of ROS production in *A. islandica* and its extreme longevity compared to closely-related bivalves. The relationships potentially linking complex I control over respiration, supercomplex robustness, and the modulation of ROS production remain to be fully assessed; our results, however, suggest that bivalves are a powerful model for this endavour.

In conclusion, we demonstrated differences in respiratory control by complex I, II, and IV in aquatic invertebrate species expressing different lifespans. To our knowledge, this study is the first to investigate the distribution of control strengths of key enzymatic complexes over mitochondrial respiration in four different species of bivalves from contrasting taxonomic groups and longevities. Our results suggest a fine regulation of the ETS in these animals, and further reinforce the idea of crucial roles for complexes I and IV in the aging phenotype where a long lifespan is associated with low control of respiration at the level of complex I, and a higher control at complex IV, with potential effects on ROS regulation. The next logical step should involve measuring the effect of ETS complex inhibition on ROS production, i.e., their individual control strength on ROS generation. Although the mitochondrial properties uncovered in this study do not necessarily cause differences in lifespan *per se*, we believe they are important hallmarks that allow species to attain high longevities.

Acknowledgments

The authors would like to thank and acknowledge the help of Amélie St-Pierre and Véronique Dérosiers for designing the experiments and gathering preliminary enzymatic activities. We are also thankful to Daniel Munro for many fruitful discussions, and to Katherine Mathers for her advice concerning the preparation of reduced CoQ_2. This research was supported by a NSERC grant to P.U.B. (RGPIN-2019-05992) and an FRQNT grant to E.R. The experimentation has been planned by E.R., P.U.B. and T.H.. The experimentations and analysis have been performed by E.R. and M.H. and

E.R. completed data analysis.. E.R., P.U.B. T.H. and H.L. participated to the interpretation of the results and the redaction of the manuscript.

Data Availability Statement

The data that support the findings of this study are available on Mendeley: (DOI: 10.17632/56rjw3bgz9.1; Rodriguez et al. 2019)

References

1. Munro D, Baldy C, Pamenter ME, Treberg JR. The exceptional longevity of the naked mole-rat may be explained by mitochondrial antioxidant defenses. Aging Cell. 2019;18(3):e12916. https://doi.org/10.1111/10.1111/acel.12916
2. Deepashree S, Niveditha S, Shivanandappa T, Ramesh SR. Oxidative stress resistance as a factor in aging: evidence from an extended longevity phenotype of Drosophila melanogaster. Biogerontology. 2019;20(4):497-513.https://doi.org/10.1007/s10522-019-09812-7
3. Blier PU, Abele D, Munro D, Degletagne C, Rodriguez E, Hagen T. What modulates animal longevity? Fast and slow aging in bivalves as a model for the study of lifespan. Semin Cell Dev Biol. 2017.http://dx.doi.org/10.1016/j.semcdb.2017.07.046
4. Stuart JA, Maddalena LA, Merilovich M, Robb EL. A midlife crisis for the mitochondrial free radical theory of aging. Longevity & Healthspan. 2014;3:4-. https://doi.org/10.1186/2046-2395-3-4
5. Barja G. Updating the mitochondrial free radical theory of aging: an integrated view, key aspects, and confounding concepts. Antioxidants & redox signaling. 2013;19(12):1420-45.https://doi.org/10.1089/ars.2012.5148
6. Butler PG, Wanamaker AD, Scourse JD, Richardson CA, Reynolds DJ. Variability of marine climate on the North Icelandic Shelf in a 1357-year proxy archive based on growth increments in the bivalve Arctica islandica. Palaeogeogr, Palaeoclimatol, Palaeoecol. 2013;373:141-51.http://dx.doi.org/10.1016/j.palaeo.2012.01.016
7. Munro D, Blier PU. The extreme longevity of Arctica islandica is associated with increased peroxidation resistance in mitochondrial membranes. Aging Cell. 2012;11(5):845-55. https://doi.org/10.1111/j.1474-9726.2012.00847.x
8. Munro D, Pichaud N, Paquin F, Kemeid V, Blier PU. Low hydrogen peroxide production in mitochondria of the long-lived Arctica islandica: underlying mechanisms for slow aging. Aging Cell. 2013;12(4):584-92.https://doi.org/10.1111/acel.12082
9. Abele D, Brey T, Philipp E. Bivalve models of aging and the determination of molluscan lifespans. Experimental Gerontology. 2009;44(5):307-15.https://doi.org/10.1016/j.exger.2009.02.012
10. Quinlan CL, Perevoschikova IV, Goncalves RL, Hey-Mogensen M, Brand MD. The determination and analysis of site-specific rates of mitochondrial reactive oxygen species production. Methods Enzymol. 2013;526:189-217.https://doi.org/10.1016/b978-0-12-405883-5.00012-0
11. Lambert AJ, Buckingham JA, Boysen HM, Brand MD. Low complex I content explains the low hydrogen peroxide production rate of heart mitochondria from the long-lived pigeon, Columba livia. Aging cell. 2010;9(1):78-91. https://doi.org/10.1111/j.1474-9726.2009.00538.x
12. Miwa S, Jow H, Baty K, Johnson A, Czapiewski R, Saretzki G, et al. Low abundance of the matrix arm of complex I in mitochondria predicts longevity in mice. Nat Commun. 2014;5. https://doi.org/10.1038/ncomms4837
13. Groen AK, Wanders RJ, Westerhoff HV, van der Meer R, Tager JM. Quantification of the contribution of various steps to the control of mitochondrial respiration. J Biol Chem. 1982;257(6):2754-7
14. Letellier T, Malgat M, Mazat J-P. Control of oxidative phosphorylation in rat muscle mitochondria: implications for mitochondrial myopathies. Biochimica et Biophysica Acta (BBA) - Bioenergetics. 1993;1141(1):58-64.https://doi.org/10.1016/0005-2728(93)90189-M
15. Murphy MP. How understanding the control of energy metabolism can help investigation of mitochondrial dysfunction, regulation and pharmacology. Biochimica et

Biophysica Acta (BBA) - Bioenergetics. 2001;1504(1):1-11.http://dx.doi.org/10.1016/S0005-2728(00)00234-6
16. Kuznetsov AV, Winkler K, Kirches E, Lins H, Feistner H, Kunz WS. Application of inhibitor titrations for the detection of oxidative phosphorylation defects in saponin-skinned muscle fibers of patients with mitochondrial diseases. Biochimica et Biophysica Acta (BBA) - Molecular Basis of Disease. 1997;1360(2):142-50.http://dx.doi.org/10.1016/S0925-4439(96)00072-5
17. Ventura B, Genova ML, Bovina C, Formiggini G, Lenaz G. Control of oxidative phosphorylation by Complex I in rat liver mitochondria: implications for aging. Biochimica et Biophysica Acta (BBA) - Bioenergetics. 2002;1553(3):249-60.http://dx.doi.org/10.1016/S0005-2728(01)00246-8
18. Sipos I, Tretter L, Adam-Vizi V. Quantitative relationship between inhibition of respiratory complexes and formation of reactive oxygen species in isolated nerve terminals. J Neurochem. 2003;84(1):112-8. https://doi.org/10.1046/j.1471-4159.2003.01513.x
19. Arnold S. The power of life--cytochrome c oxidase takes center stage in metabolic control, cell signalling and survival. Mitochondrion. 2012;12(1):46-56.https://doi.org/10.1016/j.mito.2011.05.003
20. Gosling E. Morphology of bivalves. In: Gosling E, editor. Marine Bivalve Molluscs. 2nd ed: Wiley Blackwell; 2015.
21. Moyes CD, Moon TW, Ballantyne JS. Glutamate catabolism in mitochondria from Mya arenaria mantle: Effects of pH on the role of glutamate dehydrogenase. J Exp Zool. 1985;236(3):293-301. https://doi.org/10.1002/jez.1402360306
22. Thibault M, Blier PU, Guderley H. Seasonal variation of muscle metabolic organization in rainbow trout (Oncorhynchus mykiss). Fish Physiol Biochem. 1997;16(2):139-55. https://doi.org/10.1007/BF00004671
23. Barrientos A, Fontanesi F, Díaz F. Evaluation of the Mitochondrial Respiratory Chain and Oxidative Phosphorylation System Using Polarography and Spectrophotometric Enzyme Assays. Current Protocols in Human Genetics: John Wiley & Sons, Inc.; 2009.
24. Jovanović DŠ, Đorđević M, Savković U, Lazarević J. The effect of mitochondrial complex I inhibitor on longevity of short-lived and long-lived seed beetles and its mitonuclear hybrids. Biogerontology. 2014;15(5):487-501.https://doi.org/10.1007/s10522-014-9520-5
25. Sahu S, Dattani A, Aboobaker AA. Secrets from immortal worms: What can we learn about biological ageing from the planarian model system? Semin Cell Dev Biol. 2017;70:108-21.https://doi.org/10.1016/j.semcdb.2017.08.028
26. Scott KY, Matthew R, Woolcock J, Silva M, Lemieux H. Adjustments in control of mitochondrial respiratory capacity while facing temperature fluctuations. The Journal of experimental biology. 2019:jeb.207951.https://doi.org/10.1242/jeb.207951
27. Genova ML, Pich MM, Bernacchia A, Bianchi C, Biondi A, Bovina C, et al. The mitochondrial production of reactive oxygen species in relation to aging and pathology. Ann N Y Acad Sci. 2004;1011(1):86-100.https://doi.org/10.1196/annals.1293.010
28. Pujol C, Bratic-Hench I, Sumakovic M, Hench J, Mourier A, Baumann L, et al. Succinate Dehydrogenase Upregulation Destabilize Complex I and Limits the Lifespan of gas-1 Mutant. PLoS One. 2013;8(3):e59493.https://doi.org/10.1371/journal.pone.0059493
29. Dröse S. Differential effects of complex II on mitochondrial ROS production and their relation to cardioprotective pre- and postconditioning. Biochimica et Biophysica Acta (BBA) - Bioenergetics. 2013;1827(5):578-87.https://doi.org/10.1016/j.bbabio.2013.01.004
30. Quinlan CL, Orr AL, Perevoshchikova IV, Treberg JR, Ackrell BA, Brand MD. Mitochondrial Complex II Can Generate Reactive Oxygen Species at High Rates in Both the

Forward and Reverse Reactions. J Biol Chem. 2012;287(32):27255-64.https://doi.org/10.1074/jbc.M112.374629
31. Caro P, Gomez J, Lopez-Torres M, Sanchez I, Naudi A, Jove M, et al. Forty percent and eighty percent methionine restriction decrease mitochondrial ROS generation and oxidative stress in rat liver. Biogerontology. 2008;9(3):183-96.http://dx.doi.org/10.1007/s10522-008-9130-1
32. Neretti N, Wang P-Y, Brodsky AS, Nyguyen HH, White KP, Rogina B, et al. Long-lived Indy induces reduced mitochondrial reactive oxygen species production and oxidative damage. Proceedings of the National Academy of Sciences. 2009;106(7):2277-82.https://doi.org/10.1073/pnas.0812484106
33. Dalmonte ME, Forte E, Genova ML, Giuffrè A, Sarti P, Lenaz G. Control of Respiration by Cytochrome c Oxidase in Intact Cells: ROLE OF THE MEMBRANE POTENTIAL. J Biol Chem. 2009;284(47):32331-5.https://doi.org/10.1074/jbc.M109.050146
34. Vogt S, Rhiel A, Weber P, Ramzan R. Revisiting Kadenbach: Electron flux rate through cytochrome c-oxidase determines the ATP-inhibitory effect and subsequent production of ROS. Bioessays. 2016;38(6):556-67. https://doi.org/10.1002/bies.201600043
35. Ren J-C, Rebrin I, Klichko V, Orr WC, Sohal RS. Cytochrome c oxidase loses catalytic activity and structural integrity during the aging process in Drosophila melanogaster. Biochem Biophys Res Commun. 2010;401(1):64-8.https://doi.org/10.1016/j.bbrc.2010.09.009
36. Petrosillo G, De Benedictis V, Ruggiero FM, Paradies G. Decline in cytochrome c oxidase activity in rat-brain mitochondria with aging. Role of peroxidized cardiolipin and beneficial effect of melatonin. J Bioenerg Biomembr. 2013;45(5):431-40.https://doi.org/10.1007/s10863-013-9505-0
37. Short KR, Bigelow ML, Kahl J, Singh R, Coenen-Schimke J, Raghavakaimal S, et al. Decline in skeletal muscle mitochondrial function with aging in humans. Proceedings of the National Academy of Sciences of the United States of America. 2005;102(15):5618-23.https://doi.org/10.1073/pnas.0501559102
38. Chin RM, Fu X, Pai MY, Vergnes L, Hwang H, Deng G, et al. The metabolite α-ketoglutarate extends lifespan by inhibiting ATP synthase and TOR. Nature. 2014;510:397.https://doi.org/10.1038/nature13264
39. Bettinazzi S, Rodríguez E, Milani L, Blier PU, Breton S. Metabolic remodelling associated with mtDNA: insights into the adaptive value of doubly uniparental inheritance of mitochondria. Proceedings of the Royal Society B: Biological Sciences. 2019;286(1896):20182708.http://dx.doi.org/10.1098/rspb.2018.2708
40. McDonald AE, Pichaud N, Darveau CA. "Alternative" fuels contributing to mitochondrial electron transport: Importance of non-classical pathways in the diversity of animal metabolism. Comparative biochemistry and physiology Part B, Biochemistry & molecular biology. 2018;224:185-94. https://doi.org/10.1016/j.cbpb.2017.11.006
41. Gosling E. How bivalves feed. In: Gosling E, editor. Marine Bivalve Molluscs. 2nd ed: Wiley Blackwell; 2015.
42. Orr AL, Quinlan CL, Perevoshchikova IV, Brand MD. A Refined Analysis of Superoxide Production by Mitochondrial sn-Glycerol 3-Phosphate Dehydrogenase. J Biol Chem. 2012;287(51):42921-35.https://doi.org/10.1074/jbc.M112.397828
43. Bianchi C, Genova ML, Parenti Castelli G, Lenaz G. The Mitochondrial Respiratory Chain Is Partially Organized in a Supercomplex Assembly: Kinetic Evidence Using Flux Control Analysis. J Biol Chem. 2004;279(35):36562-9.http://dx.doi.org/10.1074/jbc.M405135200
44. Gómez LA, Hagen TM. Age-related decline in mitochondrial bioenergetics: Does supercomplex destabilization determine lower oxidative capacity and higher superoxide

production? Seminars in Cell and Developmental Biology. 2012;23(7):758-67.https://doi.org/10.1016/j.semcdb.2012.04.002
45. Guo R, Gu J, Zong S, Wu M, Yang M. Structure and mechanism of mitochondrial electron transport chain. Biomedical Journal. 2018;41(1):9-20.https://doi.org/10.1016/j.bj.2017.12.001
46. Kauppila TES, Kauppila JHK, Larsson N-G. Mammalian Mitochondria and Aging: An Update. Cell Metabolism. 2017;25(1):57-71.https://doi.org/10.1016/j.cmet.2016.09.017
47. Jang S, Javadov S. Elucidating the contribution of ETC complexes I and II to the respirasome formation in cardiac mitochondria. Sci Rep. 2018;8(1):17732.https://doi.org/10.1038/s41598-018-36040-9

Figure legends

Figure 1. (A) Schematic coupling control/pathway state diagram illustrating the five substrate, uncouplers and inhibitor titrations (SUIT) protocols used in the study. Each section shows protocols for the NADH (N), Succinate (S), Complex III (CIII), Complex IV-pathways and combined NSGp-pathway, respectively. G: glutamate, M: malate, Gp: glycerol-3-phosphate, D: ADP, U: FCCP, Rot: rotenone, Mna: malonate, Ama: antimycin a, nPG: n-propyl gallate, AsTm: Ascorbate and TMPD, KCN: potassium cyanide, Inh: inhibitors (one of the aforementioned), while asterisks indicate multiple-step titrations. For further details please refer to the methods section. (B) Flux control ratios normalized for NSGp-linked pathway capacity in isolated mitochondria from 4 species of marine bivalves. Box plots show minimum, 25th percentile, median, 75th percentile, and maximum for 3 species: *M. arenaria*, *S. solidissima*, and *M. mercenaria*, while *A. islandica* means are represented as filled triangles (*n* = 3-5 individuals per species). (C) Contribution of NADH (N-), succinate (S-) and glycerol-3-phosphate (Gp-) pathways to oxidative phosphorylation in 4 species of marine bivalves. Box plots show minimum, 25th percentile, median, 75th percentile, and maximum. Contributions are calculated for N: N/NSG_p, S: $(NS - N)/ NSG_p$, and for Gp: $(NSG_p - NS)/ NSG_p$ (*n* = 4-5 individuals per species). Letters denote significant ($p \leq 0.05$) differences among states-FCRs.

Figure 2. Relative NSGp-pathway flux as a function of relative N-pathway (A) or S-pathway (B) inhibition in 4 species of short- to long-lived marine bivalves: *M. arenaria* (black), *S. solidissima* (gray), and *M. mercenaria* (blue), *A. islandica* (red). Data are presented as means ±SEM (*n* = 4-5). For detailed titration curves of the isolated pathways for each species, please refer to figures S1 and S2 in the supplementary information.

Figure 3. Relative NSGp-pathway flux as a function of relative complex IV inhibition in each of the 4 species of short- to long-lived marine bivalves: *M. arenaria* (A, black), *S. solidissima* (B, gray), and *M. mercenaria* (C, blue), *A. islandica* (D, red). Open circles show data up to the threshold of inhibition, and the CIV_E / NSGp flux ratio is calculated as the intercept at zero CIV inhibition of a linear regression through the points after the inhibition threshold. Data are presented as means ±SEM (*n* = 4-5). For detailed titration curves of the single step and the combined pathway for each species, please refer to figure S4 in the supplementary information.

Figure 4. Stacked bars showing flux control coefficients for N-, S-, CIII- pathways and CIV single step (and sums thereof) in 4 species of short- to long-lived marine bivalves. Letters denote significant ($p \leq 0.05$) differences among species. Data are presented as means (*n* = 4-5 individuals per calculated coefficient, per species).

Figure 1

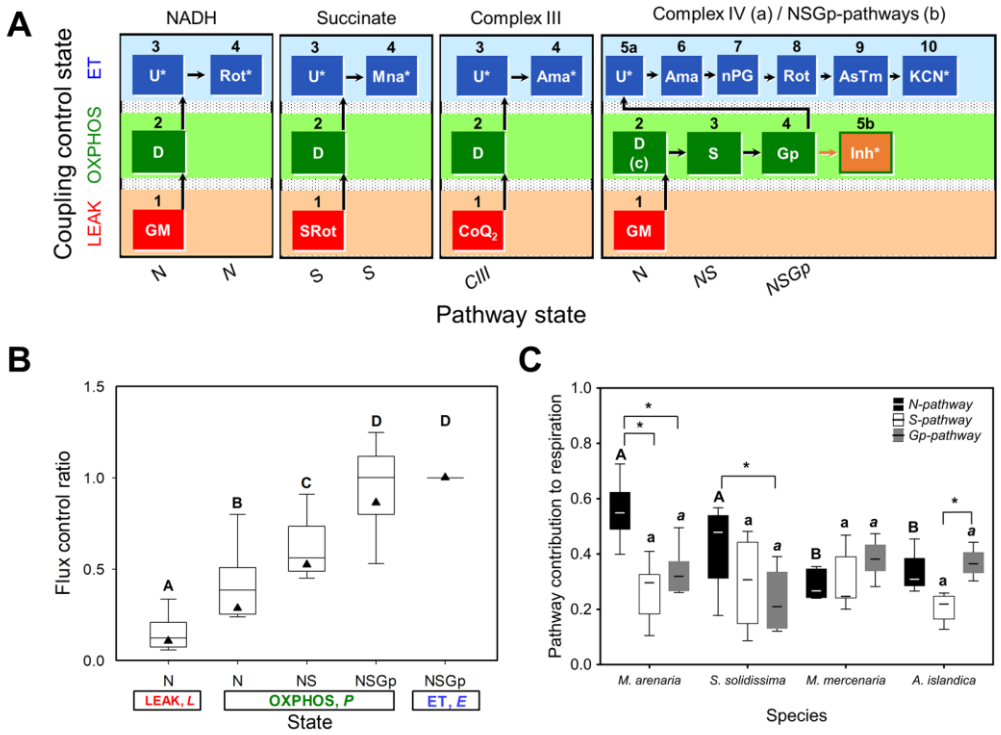

Figure 2

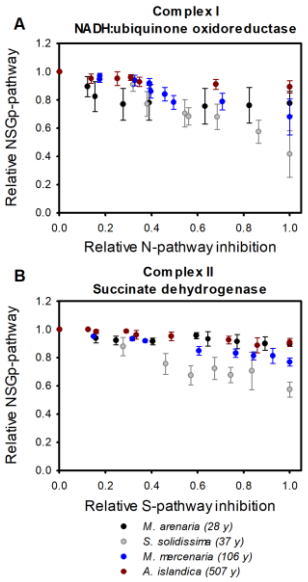

Figure 3

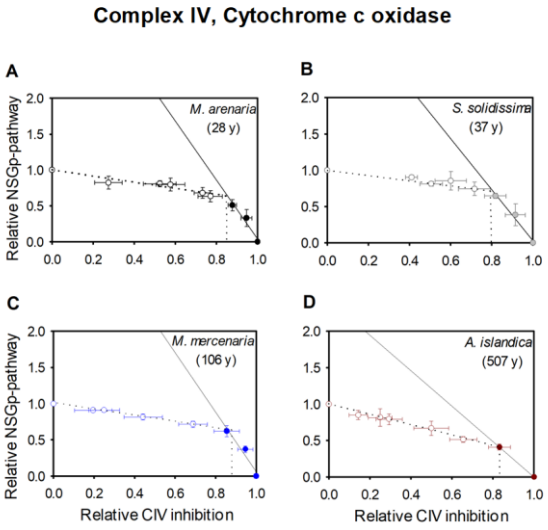

Figure 4